Electronic Supplementary Material (ESI) for Nanoscale.

Supplementary Information

3D Intra-Stacked CoO/Carbon Nanocomposites Welded by Ag Nanoparticles for High-Capacity, Reversible Lithium Storage

Changju Chae,[a] Ki Woong Kim,[a] Sue Jin Kim,[a] Daehee Lee,[b] Yejin Jo,[a] Young Jun Yun,[a] Jooho Moon,[b] Youngmin Choi,[a] Sun Sook Lee,[a,*] Sungho Choi,[a,*] Sunho Jeong[a,*]

[a]Division of Advanced Materials, Korea Research Institute of Chemical Technology (KRICT), Daejeon 305-600, Republic of Korea

E-mail: sunsukl@krict.re.kr; shochoi@krict.re.kr; sjeong@krict.re.kr

[b]Department of Materials Science and Engineering, Yonsei University, 50 Yonsei-ro Seodaemun-gu, Seoul 120-749, Republic of Korea

Table S1. Details for C 1s core level spectra of as-prepared and thermally annealed 3D-NCs

	Before annealing[a]		After annealing	
	binding energy (eV)	fraction (%)	binding energy (eV)	fraction (%)
C-C	284.4	28.8	284.5	68.2
C-O	285.2	13.2	285.4	11.2
C-O-C	286.6	29.4	286.5	10.1
C=O	288.1	16.1	288.1	5.3
O-C=O	289.2	8	289.3	3
π-π*	290.7	4.5	290.8	2.2

[a]Thermal annealing was carried out at 300 ^{o}C.

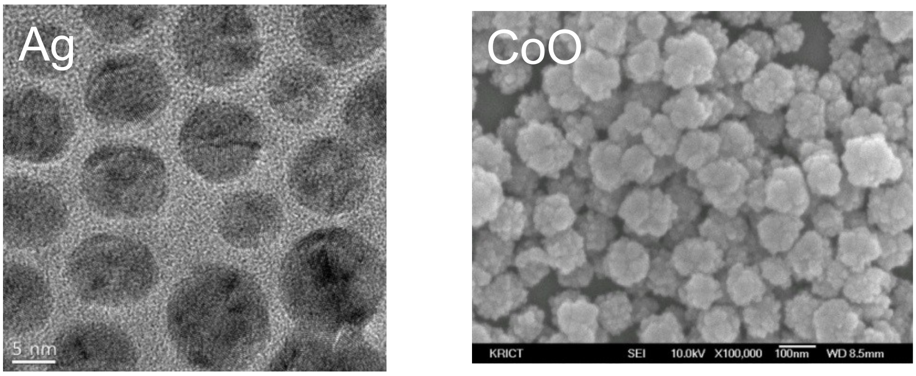

Figure S1. (a) HRTEM image of Ag nanoparticles and (b) SEM image of CoO nanoparticles

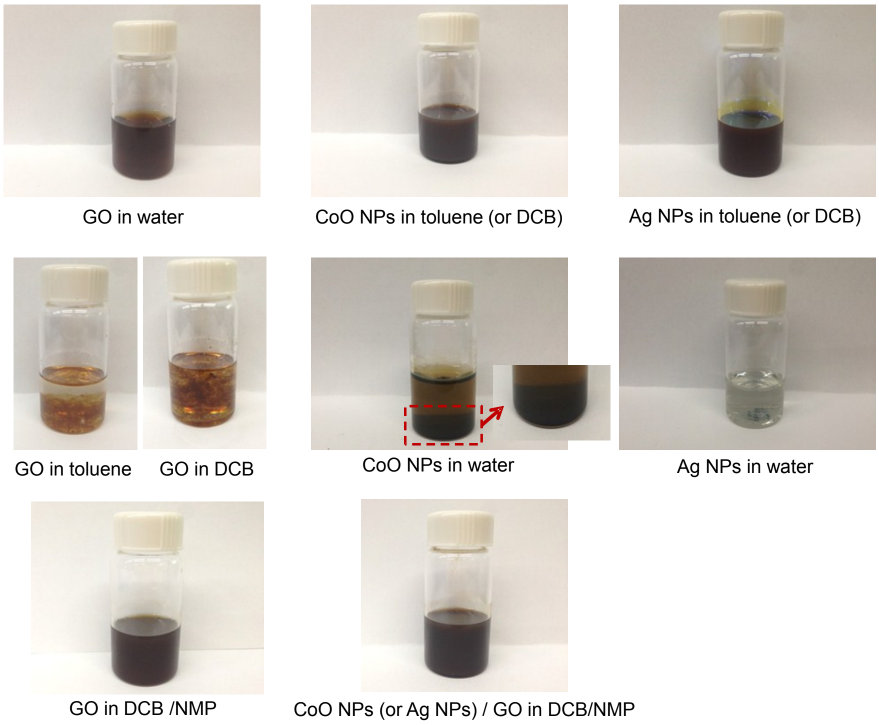

Figure S2. Photographs showing the miscibility/immiscibility of GO, CoO nanoparticles, and Ag nanoparticles in various solvents. The concentration for all suspensions was 20 mg/ml.

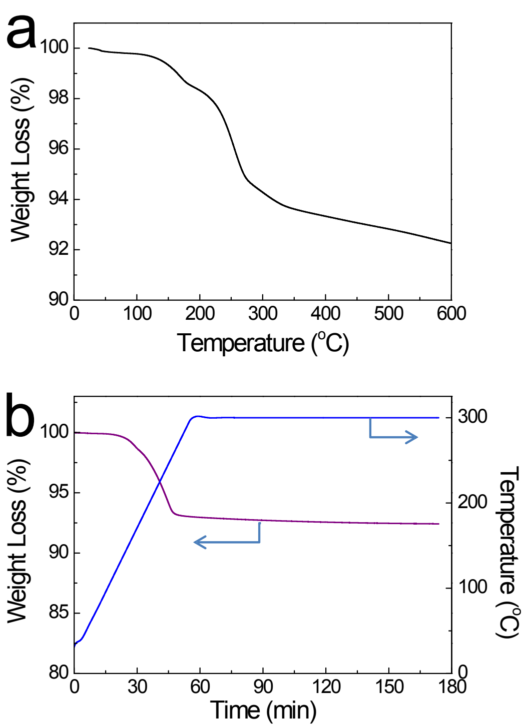

Figure S3. TGA results for synthesized Ag nanoparticles under Ar gas: (a) Thermal behavior as a function of temperature and (b) thermal behavior as a function of time at 300 °C

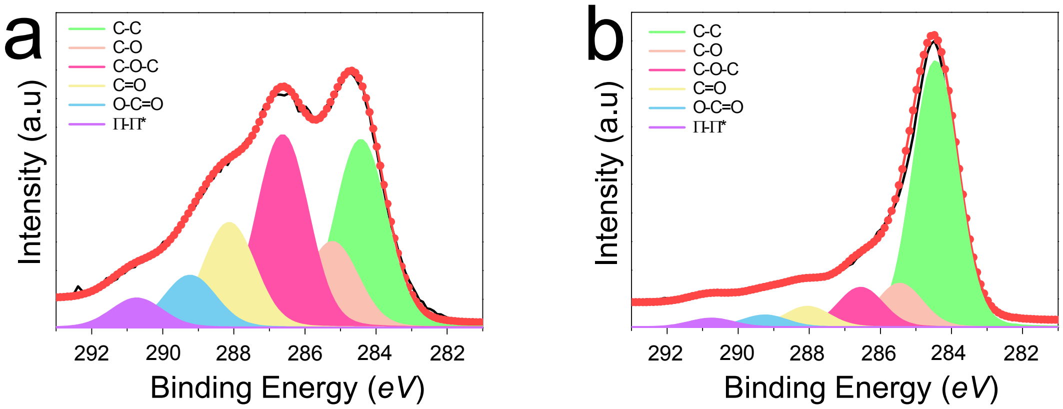

Figure S4. XPS C 1s spectra for (a) as-prepared and (b) thermally annealed 3D-NCs. The thermal annealing was carried out at 300 °C under Ar gas.

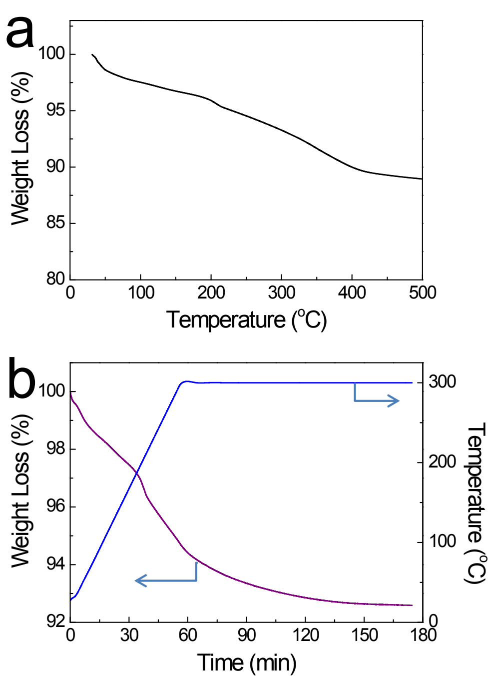

Figure S5. TGA results for synthesized CoO nanoparticles under Ar atmosphere: thermal behavior as a function of (a) temperature and (b) time at 300 °C

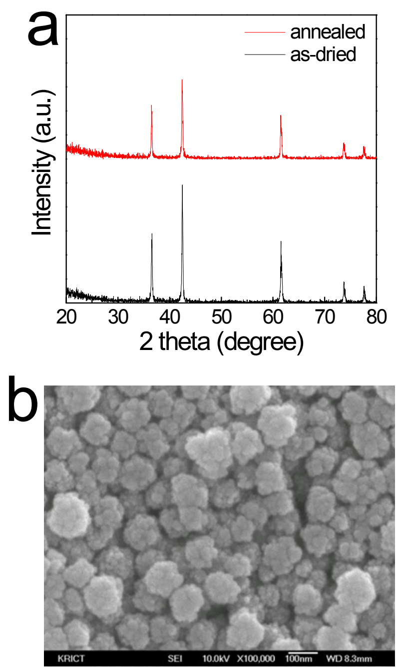

Figure S6. (a) X-ray diffraction results for as-synthesized and thermally annealed CoO nanoparticles and (b) SEM image for thermally annealed CoO nanoparticles. The thermal annealing was carried out at 300 °C under Ar atmosphere.

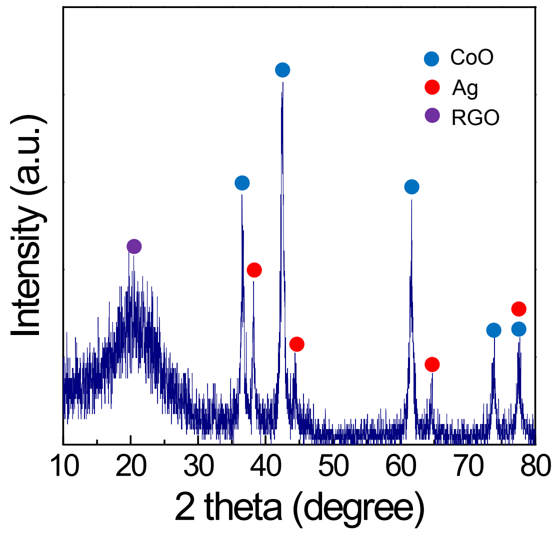

Figure S7. X-ray diffraction result for CoO/Ag/RGO nanocomposite with composition of 80 (CoO): 8 (Ag): 12 (GO) wt%.

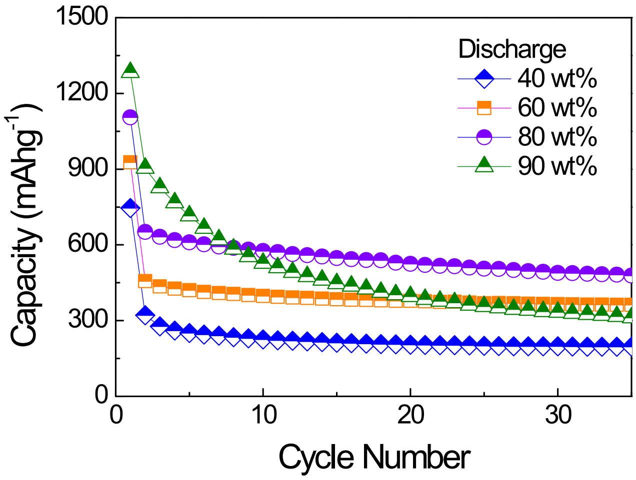

Figure S8. Cycling performance for composite electrodes employing 3D-NCs with different proportions of CoO nanoparticles at a current density of 100 mA/g. In the batches for mixing Ag nanoparticles, CoO nanoparticles, and graphene oxides, the proportion of CoO was varied from 40 to 90 wt%, while the weight ratio of Ag to GO was maintained at 8/12.

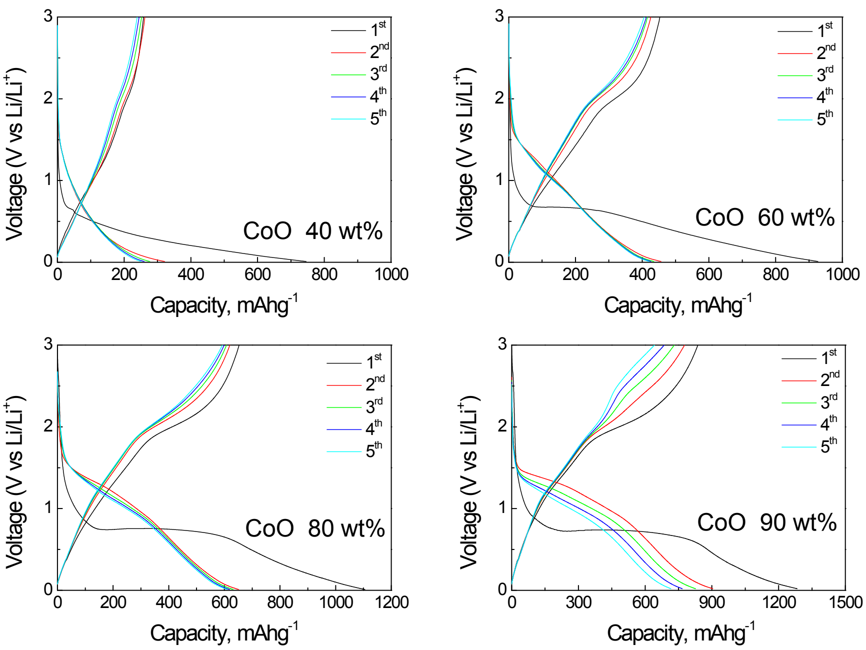

Figure S9. Voltage profiles for composite electrodes with 3D-NCs, with different proportions of CoO nanoparticles, at a current density of 100 mA/g. In the batches for mixing Ag nanoparticles, CoO nanoparticles, and graphene oxides, the proportion of CoO was varied from 40 to 90 wt%, while the weight ratio of Ag to GO was maintained at 8/12.

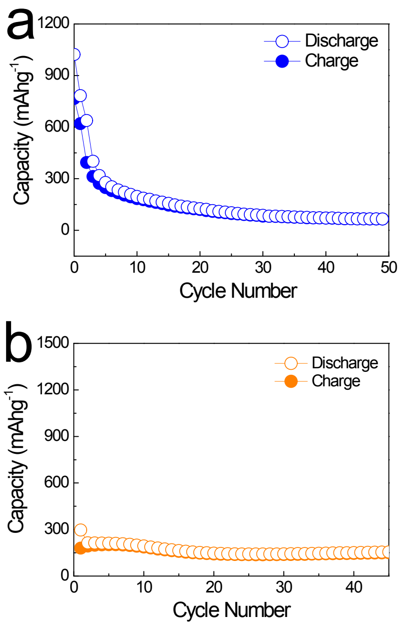

Figure S10. Cycling performance for composite electrodes containing (a) CoO nanoparticles and (b) Ag nanoparticles at a current density of 100 mA/g.

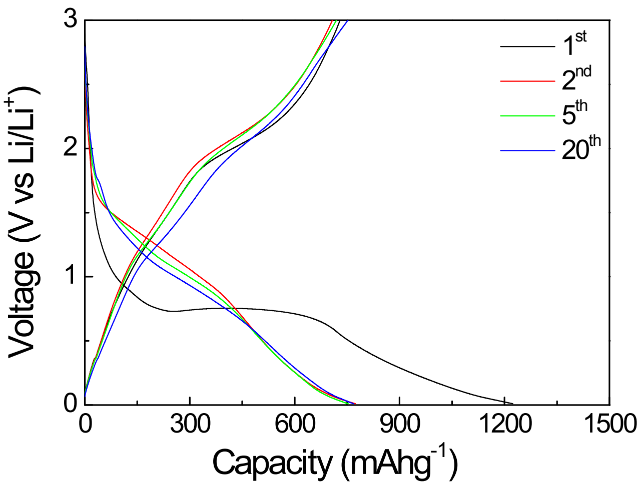

Figure S11. Voltage profiles for electrodes containing MWCNT (1 wt%)-incorporated 3D-NC at a current density of 100 mA/g.

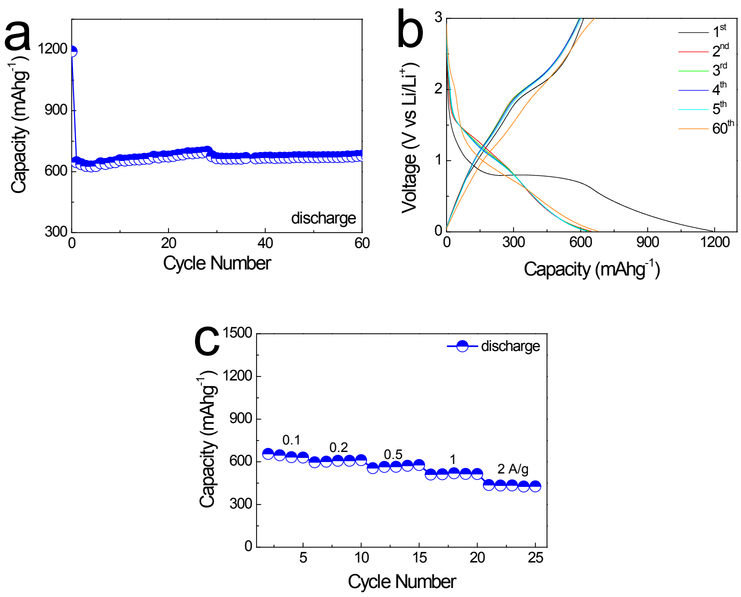

Figure S12. (a) Cycling performance at a current density of 100 mA/g, (b) voltage profiles at a current density of 100 mA/g, and (c) rate performance for electrodes employing MWCNT-incorporated Ni/CoO/RGO composite materials

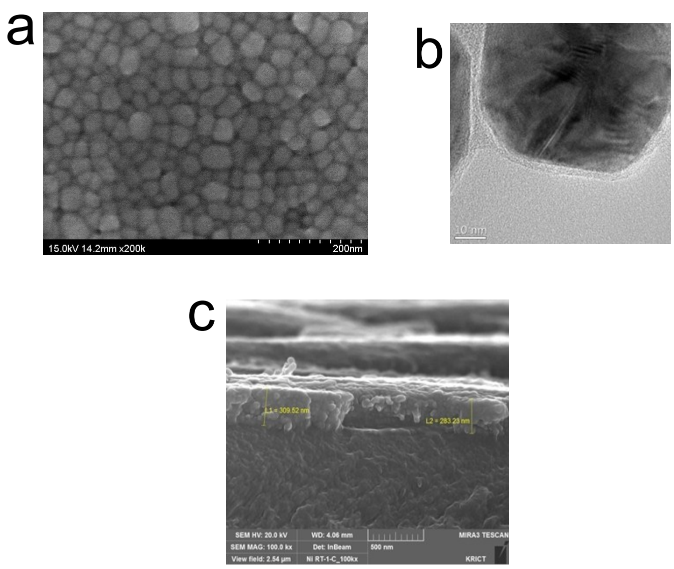

Figure S13. (a) SEM and (b) HRTEM images of Ni nanoparticles synthesized in this study. In the HRTEM image, the shell layer present on the surface of the Ni nanoparticles is attributable to capping molecules and surface oxide layer. (c) SEM image of Ni nanoparticle film prepared by drop casting the Ni nanoparticle suspension, after a thermal annealing at 400 ^{o}C under Ar atmosphere.